Mutual Impacts and Interactions of Antibiotic Resistance Genes, Microcystin Synthetase Genes, Graphene Oxide, and Microcystis Aeruginosa in Synthetic Wastewater

Shichao Wu
Shanghai Institute of Technology
Xiyan Ji (xiyanji@sit.edu.cn)
Shanghai Institute of Technology
Xin Li
Shanghai Institute of Technology
Jing Ye
Shanghai Institute of Technology
Wenwu Xu
Shanghai Institute of Technology
Rui Wang
Shanghai Majorbio. Tec. Ltd
Meifang Hou
Shanghai Institute of Technology

Research Article

Keywords: Interactions, Antibiotic resistance genes, Microcystin synthetase gene, Microcystic aeruginosa, Graphene oxide

Posted Date: May 21st, 2021

DOI: https://doi.org/10.21203/rs.3.rs-322632/v1

Version of Record: A version of this preprint was published at Environmental Science and Pollution Research on August 16th, 2021. See the published version at https://doi.org/10.1007/s11356-021-15627-2.

Mutual impacts and interactions of antibiotic resistance genes, microcystin synthetase genes, graphene oxide, and *Microcystis aeruginosa* in synthetic wastewater

Shichao Wu[1], Xiyan Ji[1*], Xin Li[1], Jing Ye[2], Wenwu Xu[3], Rui Wang[4], Meifang Hou[1*]

[1] School of Ecological Technology and Engineering, Shanghai Institute of Technology, Shanghai 201418, P.R. China

[2] School of Chemical and Environmental Engineering, Shanghai Institute of Technology, Shanghai 201418, P.R. China

[3] School of Railway Transportation, Shanghai Institute of Technology, Shanghai 201418, P.R. China

[4] Shanghai Majorbio Bio-Pharm Technology Co., Ltd, Shanghai 201318, P.R. China

*Corresponding authors:

Dr. Xiyan Ji, E-mail: xiyanji@sit.edu.cn

Prof. Meifang Hou, E-mail: mfhou@sit.edu.cn

Abstract

The physiological impacts and interactions of ARGs abundance, microcystin synthetase genes expression, GO, and *M. aeruginosa* in synthetic wastewater were investigated. The results demonstrated that the absolute abundance of *sul1*, *sul2*, *tetW*, and *tetM* in synthetic wastewater dramatically increased to 365.2%, 427.1%, 375.2%, and 231.7%, respectively, when the GO concentration was 0.01 mg/L. Even more interesting is that the sum gene copy numbers of *mcyA-J* also increased to 243.2%. The appearance of GO made the significant correlation exist between ARGs abundance and *mcyA-J* expression. Furthermore, *M. aeruginosa* displayed better photosynthetic performance and more MCs production at 0.01 mg/L GO. There were 65 pairs of positive correlations between the intracellular differential metabolites of *M. aeruginosa* and the abundance of *sul1*, *sul2*, *tetM*, and *tetW* with various GO concentrations. The GO will impact the metabolites and metabolic pathway in *M. aeruginosa*. The metabolic changes impacted the ARGs, microcystin synthetase genes, and physiological characters in algal cells. Furthermore, there were complex correlations among *sul1*, *sul2*, *tetM*, *tetW*, *mcyA-J*, MCs, photosynthetic performance parameters, and ROS. The different concentration of GO will aggravate the hazards of *M. aeruginosa* by promoting the expression of *mcyA-J*, producing more MCs, simultaneously, it may cause the spread of ARGs.

Keywords: Interactions, Antibiotic resistance genes, Microcystin synthetase gene, *Microcystic aeruginosa*, Graphene oxide

1. Introduction

Antibiotic resistance genes (ARGs) pollution has become knotty problem that has attracted much attention around the world (Conley et al. 2009). The overuse of antibiotics in medicine, cultivation, and aquaculture field has caused the accumulation of ARGs in aquatic environment (Komijani et al. 2021). The ARGs have been detected in many water bodies in China, especially ARGs of sulfonamides and tetracyclines are ubiquitous and with high concentration (Sun et al. 2017). The average level of ARGs in natural waters reached 1.2×10^8 gene copies/mL (Sun et al. 2017). There are not only large amounts of ARGs remaining in general water bodies, but also the problem of *Microcystis aeruginosa* (*M. aeruginosa*) should not be ignored. The overgrowth of *M. aeruginosa* not only caused harmful algae bloom but also produced very potent microcystins (MCs) which can stimulate oxidative stress of the cell, which would produce a large amount of reactive oxygen species (ROS) (Chen et al. 2016, McLellan &Manderville 2017). The ROS would promote the change of cell permeability, which accelerate the release of intracellular substances (Jiang et al. 2021). The increase in membrane permeability is one of the fundamental reasons for increasing the transfer efficiency of ARGs (Guo et al. 2021, Lu et al. 2020b, Sun et al. 2018). And then, to make matters worse, the graphene oxide (GO) would inevitably be released into the aquatic environment with its extensive application (Yang et al. 2019, Zhu et al. 2019). The presence of GO might have a certain impact on the growth of *M. aeruginosa*, microcystin synthetase genes, and MCs production (Yang et al. 2019). Aquatic environment is an important medium for the release and diffusion of MCs, ARGs, and GO. These pollutants can invade the human food chain by the water cycle, posing a serious threat to the aquatic ecological environment and human health (Avant et al. 2019, Jiang et al. 2020).

It is known that the pollutants in natural water bodies are very complicated, and there are many kinds of pollutants such as ARGs, *M. aeruginosa*, and nano-pollutants (Rzymski et al. 2020). The GO might affect the microcystin synthetase genes expression and MCs production when its concentration reaches a certain level (Wang et al. 2020a, Yin et al. 2020). People formerly believed

that the abuse of antibiotics was the main reason for global accumulation and spread of ARGs (Sola 2020). However, more and more studies have shown that natural-occurring substances and some kinds of nano-pollutants in the aquatic environment can promote the spread of ARGs (Sun et al. 2021). Studies have shown that extractive of *M. aeruginosa* and pure MCs and nanometer materials can cause the spread of ARGs in aquatic environment (Fan et al. 2021, Xu et al. 2021). Some researchers have inferred that MCs and nanometer materials might change the permeability and surface functional groups of microbial cells and accelerate the rate which ARGs genetic material enters cells (Fan et al. 2021).

MCs are synthesized by the megazyme complex through non-ribosomal pathways (Yang et al. 2015). This type of complexus includes peptide synthase, polyketide synthase and some other modified enzymes (Wei et al. 2020). By sequencing the gene cluster encoding synthase, it was found that the gene cluster contained a type of mixed non-ribosomal peptide synthetase genes including *mcyA*, *mcyB*, *mcyC*, *mcyD*, *mcyE*, *mcyF*, *mcyG*, *mcyH*, *mcyI* and *mcyJ* (Lu et al. 2020a). Simultaneously, nano-pollutants in aquatic environment will also affect the production of MCs. In the presence of GO, the transcription levels of the synthetase genes *mcyA*, *mcyB* and *mcyD* are significantly increased (Grasso et al. 2020). Therefore, what can be inferred is that although the production of MCs is determined by the genes in the microcystin-producing cells, the nano-pollutants such as GO in environment can also regulate their gene expression, thereby affecting the synthesis of MCs. The presence of MCs may increase the abundance of ARGs, and the GO in the aquatic environment might make the transcription of MCs synthase genes increase. While, there is still no result that can effectively verify this inference, this work is trying to prove this. What are the mutual impacts and interactions of ARGs, microcystin synthetase genes, MCs, GO, and *M. aeruginosa*, the researches on this aspect were currently rare.

The abundance changes of ARGs including *sul1*, *sul2*, *tetW*, *tetM* and the gene copy numbers of MCs microcystin synthetase genes including *mcyA*, *mcyB*, *mcyC*, *mcyD*, *mcyE*, *mcyF*, *mcyG*, *mcyH*, *mcyI*, *mcyJ* in GO-exposed *M. aeruginosa* with different concentrations were investigated in this study. Meanwhile, the correlativity between ARGs abundance and *mcyA-J* expression quantity was evaluated. Moreover, the effect of GO with different concentrations on the

ultrastructure, photosynthesis, metabonomics characters of *M. aeruginosa* were also studied. These results will reveal the mutual impacts and interactions of ARGs, microcystin synthetase genes, graphene oxide, and Microcystis aeruginosa in synthetic wastewater, which will provide some basics for the studies of multi-component pollutants in aquatic environment.

2. Materials and methods

2.1 Experimental design

M. aeruginosa (FACHB-315) was purchased from the Institute of Wuhan Hydrobiology, Chinese Academy of Sciences and cultured in pH 7.0 BG11 medium (**Table** S1). The GO was purchased from the Chengdu Institute of Organic Chemistry, Chinese Academy of Sciences. The GO sheets diameter was 0.1-10 μm in size with average thickness of 1.5 μm. The plasmids of ARGs including *sul1*, *sul2*, *tetW*, *tetM* were prepared by Genesis Biotechnology Co., Ltd. The gene sequences of *sul1*, *sul2*, *tetW*, *tetM* were listed in **Table** S2.

For the incubation experiment, photobioreactors as shown in **Fig**. 1 was used. The GO particles were dispersed in synthetic wastewater (**Table** S3) with initial concentrations of 0, 0.01, 0.1, 1, and 10 mg/L, and for the control group, the GO concentration was 0 mg/L. The GO concentration range was set close to that found in natural water (Zhao et al. 2020b). In these systems, GO particles had hydrodynamic diameters of 250-300 nm and zeta potentials ranges from -30 to 50 mV, indicating that the GO particles had been stably dispersed in the synthetic wastewater at the four concentrations (Monteil et al. 2014). *M. aeruginosa* was inoculated at density of 1.0×10^5 cells/mL and the reactors were placed in an illumination incubator (MGC-300A, China) at 28.0 ± 0.5°C and 75% humidity. At the beginning (0 h) and after 0, 24, 48, 96 h of incubation, samples were taken from each reactor and centrifuged at 8000×*g* for 10 min. The supernatants were used for analyses of ARGs abundance, total nitrogen (TN), ammoniacal nitrogen (NH_3-N), phosphate phosphorus (PO_4^{3-}-P), chemical oxygen demand (COD), and extracellular MCs (MC-LR and MC-RR). The precipitates were collected for intracellular MCs and reactive oxygen species (ROS) quantification, metabolic responses, *mcyA-J* gene expression analyses, and transmission electron

microscopy (TEM) observation. Only samples taken at the end of the experiment (96 h) from the control, 0.01, and 10 mg/L GO were used for metabonomic analysis.

2.2 Measurement of ARGs abudance

The ARGs abundances of *sul1*, *sul2*, *tetW*, *tetM* were measured by HT-qPCR. The Light Cycler 480 YSBR Green I Master was used as fluorochrome. A total of 14 pairs of primers were selected, including 4 ARGs primers, 10 pairs of microcystin synthetase genes primers (**Table** S2). The HR-qPCR reaction system consists of 12.5 μL PCR reaction mixture with ROX reference dye, 0.5 μL (with concentration of 10 μmol/L) forward and reverse primers, 10.5 μL DNA-free water, and 10 μL sample DNA. The operation steps of HT-qPCR were as shown as follows: ① 50℃, 2 min; ② 95℃, 5 min; ③ 95℃, 20 s; ④ annealing for 30 s; ⑤ 72℃, 30 s; ⑥ plate read, repeat the temperature of ③-⑤; ⑦ melting curve analysis, between 60-95℃, read every 0.2℃ (Wu et al. 2020a).

2.3 Measurement of algal photosynthetic response and growth rate

The phytoplankton classification fluorometer (Phyto-PAM, Germany, WALZ) was used to measure the various parameters of chlorophyll fluorescence. The specific steps are as follows: ① Start the Phyto Win software, place a certain amount of sample (the volume should be uniform each time) in a cuvette for 15 min. ②Start the instrument to determine the initial measurement fluorescence yield (F_0), measure the maximum fluorescence yield (F_m) after the saturation pulse at 4000 μmol/(m^2·s). ③ Calculate the maximum light energy conversion efficiency (F_v/F_m). ④Set the photochemistry intensity at 3 000 μmol/(m^2·s) and irradiate for 1 min util the indicator light turns green, the initial fluorescence (F_s) and maximum fluorescence (F_m') were measured when the fluorescence value was stable. The measured chlorophyll fluorescence parameters are F_0, F_m, F_0', F_m', F_s. The fluorescence parameters such as F_v/F_m, F_v/F_0, ETR_{max} were calculated as follows (Poudyal et al. 2019):

Maximum light conversion efficiency **Eq**. (1): $\frac{F_v}{F_m} = \frac{F_m - F_0}{F_m}$

Maximum photochemical quantum yield **Eq**. (2): $\frac{F_v}{F_0} = \frac{F_0}{F_m - F_0}$

Efficiency of light energy conversion **Eq**. (3): $\varphi PSII = \frac{F_m' - F_s}{F_m'}$

Quantum efficiency **Eq**. (4): $Yield = \frac{F_m' - \frac{1}{\frac{1}{F_q} - \frac{1}{F_m} - \frac{1}{F_m'}}}{F_m'}$

Photosynthetic electron transport **Eq**. (5): $ETR = \varphi PSII \times DAR \times 0.5 \times 0.84$

The specific growth rate of algae is used to reflect the growth of *M. aeruginosa*. The formula is shown in **Eq**. (6):

$$\mu = \frac{\ln\left(\frac{X_n}{X_{n-1}}\right)}{t_n - t_{n-1}}$$

In **Eq**. (6): X_n is for the cell density of *M. aeruginosa* at the end of the GO-exposure period (t_n), X_{n-1} is the cell density of *M. aeruginosa* at the GO-exposure period (t_{n-1}) (Elser et al. 2007).

2.4 N, P nutrients removal determination

After the supernatants of samples were filtered through 0.44-μm filters, the concentration of nitrogen and phosphorus nutrients including TN, NH_3-N, PO_4^{3-}-P, and COD were determined as described in their study (Ajayan et al. 2019).

2.5 MCs quantification and microcystin synthetase genes expression measurement

The MCs in the supernatants were extracted with Oasis HLB and determined by liquid chromatography-mass spectrometry (LC-MS). Intracellular MCs (MC-LR and MC-RR) extraction was performed as described in previous study (Pinheiro et al. 2016). The sample was extracted with 75% methyl alcohol at 25°C for 20 min while stirring. The homogenate was centrifuged (10000×*g*, 10 min) to remove the pellet. The MCs in the supernatant were eluted using 80% (v/v)

methyl alcohol, concentrated at 35℃ (Pinheiro et al. 2016), purified, and quantified using HPLC (Agilent 1200, USA). A reversed phase column equipped with a guard column at 45℃ was used. For *mcyA-J* gene expression analysis, total RNA of *M. aeruginosa* was transcribed to cDNA for RT-qPCR analysis on a real-time PCR system (Thermo fisher, Step One Plus, USA). The qPCR amplification procedure was operated as Lee reported (Lee et al. 2020).

2.6 TEM observation and ROS determination

The algal cells of *M. aeruginosa* were added to 2.5% glutaraldehyde with the final concentration was 2.5%, then fixed for 3 h. Centrifuged at 5000×g, the supernatant was removed, and 0.1 mol/L phosphate buffer was added to wash the samples for 3 times. Then 4% osmic acid was added to fix the algal cell. The samples were centrifuged at 5000×g for 5 min after incubation overnight at 4℃, then the supernatant was removed. The acetone solutions of different concentrations of 10%, 30%, 50%, 70%, 90% and 100% were used to dehydrate. Resin was used to embed, then the sample was sectioned (EMUC7, Lycra, Austria). The 3% uranyl acetate and 2% lead citrate were used to stain. Finally, the samples were observed by transmission electron microscope (HT7700, Hitachi, Japan) (Soares et al. 2020). The ROS levels of samples were detected by ROS kit (ML Elisa0255, R&D Systems, USA) according its operating manual.

2.7 Metabonomic determination

Extraction, derivatization and GC-MS detection process of metabolites were performed as the modified method of Weckwerth (Weckwerth et al. 2004). A certain amount of sample (Grinded in liquid nitrogen) was added in 1mL pre-cooled extraction solution (volume ratio of methanol to water is 1:1) and 5 μL internal standard substance. Then the mixture was vortexed for 3 min. After centrifugation (8000×g, 5 min), 500 μL supernatant was placed in liquid nitrogen for 30 min, then the sample was freeze-dried. The 50 μL methoxyammonium hydrochloride/pyridine solution (20 mg/mL) was added, kept reacting at 40°C for 60 min. The 80 μL N-methyl-N-(trimethylsilane) trifluoroacetamide (MSTFA) was added, then reacted 80 min at 40℃. After centrifugation at 8000×g, for 10 min, the supinate was used to detection and analyzed by GC-MS.

183 **2.8 Statistical analysis**

184 The treatments and measurements were all performed in triplicate. Origin 8.5 was used for data
185 processing for statistical analysis. The identification of metabolites was performed by the NIST
186 database (2011). The metabolite data were normalized, then they were imported into SIMCA
187 software (Version 11.5) for the PCA and PLS analysis. The HCE 3.5 software was used to perform
188 hierarchical cluster analysis. The figures in this study were drawn by Graph pad Prisim 7.0.

189 **3. Results and discussion**

190 **3.1 Analysis of mutual impacts between ARGs and microcystin synthetase genes expressions**

191 The absolute abundance of the total ARGs including *sul1*, *sul2*, *tetW*, *tetM* of GO-exposed *M.*
192 *aeruginosa* systems at concentration of 0.01 mg/L was improved 4 times than that at concentration
193 of 0 mg/L, especially for *sul1*, *sul2*. The highest abundance of *sul1* and *sul2* in GO-exposed *M.*
194 *aeruginosa* system with concentration of 0.01 mg/L reached 4.14×10^{11} copies/L. The total genes
195 copies of microcystin synthetase genes including *mcyA-J* reach up to 2.98×10^{10} when the
196 concentration of GO was 0.01 mg/L. In order to explain the impacts between ARGs (*sul1*, *sul2*,
197 *tetM*, *tetQ*) and microcystin synthetase genes (*mcyA-J*), the correlation analysis was performed
198 and the results were shown in **Fig**. 2.

199 The *Pearson* correlation analysis was performed between the expression of *sul1*, *sul2*, *tetW*,
200 *tetM* and the intracellular *mcyA-J* of *M. aeruginosa* in the synthetic wastewater when GO with
201 concentration of 0.01, 0.1, 1, 10 mg/L. The results demonstrated that there were 30 pairs, 30 pairs,
202 30 pairs, and 25 pairs of correlations ($p<0.05$) between ARGs and *mcyA-J* at 24h, 48h, 72h, 96h,
203 respectively. It can be inferred that there was a positive correlation between the abundance of
204 ARGs and the expression of *mcyA-J* when the GO was present. When the GO concentration is 0,
205 there is no correlation between the abundance of *sul1*, *sul2*, *tetM*, *tetW* and *mcyA-J*, which further
206 demonstrated that the presence of GO made the abundance of ARGs closely related to the
207 expression of *mcyA-J*. Interestingly, when the concentration of GO was 0.01 mg/L, the expression

of *mcyA-J* was significantly increased ($P<0.05$), and the MCs production was also significantly increased, and the expressions of *sul1*, *sul2*, *tetM*, *tetW* were also increases significantly ($P<0.05$). The presence of GO at the concentration of 0.01 mg/L made the positive correlation between ARGs (*sul1*, *sul2*, *tetM*, *tetW*) abudance and *mcyA-J* expression further enhanced. What would be mentioned in latter section was that the photosynthesis performance of *M. aeruginosa* and MCs production were promoted when the GO concentration was 0.01 mg/L. It can be inferred that the presence of GO in aquatic environment will aggravate the overgrowth of *M. aeruginosa*, MCs production, and spread of ARGs to a certain extent (Pan et al. 2015, Wu et al. 2020b).

3.2 Influence of GO on the N, P removal by *M. aeruginosa*

The nitrogen and phosphorus nutrients including total nitrogen (TN), ammoniacal nitrogen (NH_3-N), phosphate (PO_4^{3-}-P), and chemical oxygen demand (COD) removal by *M. aeruginosa* is closely related to the growth rate (Ma et al. 2014). The removal rates of TN, NH_3-N, PO_4^{3-}-P, and COD were 25%, 72%, 36.2%, and 42.9%, respectively, at 0.01 mg/L GO exposure (**Fig**. 3), indicating that 0.01 mg/L GO-exposure can effectively stimulate and promote nutrients removal by *M. aeruginosa* from the growth environment (Aphale et al. 2015). Much smaller removals of TN, NH_3-N, PO_4^{3-}-P, and COD were observed in the 10 mg/L GO treatment, which might be attributed to the negative effects of GO at high concentration on the photosynthetic rates of algal cells [40], as evident by the low F_v/F_m and ETR_{max} demonstrated in **Fig**. 1. Simultaneously, high concentration of 10 mg/L GO inhibited nutrients removal by *M. aeruginosa* (Zhao et al. 2020a).

3.3 Cellular impacts of *M. aeruginosa* and GO

Significant effects ($p<0.05$) of GO on photosynthesis of *M. aeruginosa* was observed during the GO-exposure period at concentrations of 0.01, 0.1, 1, and 10 mg/L, respectively. The different concentration of GO-exposure also affected the growth rate significantly ($p<0.05$). The results indicated that the intracellular production and extracellular release of MCs in GO-exposed groups were higher than that in the control (without GO exposure). As shown in **Fig**. 4A, the intracellular MCs production in *M. aeruginosa* of the 0.01mg/L GO-exposure group was the highest among all

groups during the whole exposure period. Simultaneously, the number of gene copies of *mcyA-J* in the *M. aeruginosa* were the highest among all groups, indicating that the presence of GO at concentration of 0.01 mg/L stimulated the expression of microcystin synthetase genes clusters (**Fig**. 4B). This led to a significant increase ($p<0.05$) in the production of intracellular MCs. Since MCs are synthesized intracellularly and are released to extracellular when the algal cell ruptured (Rincon et al. 2019), the percentage of extracellular MCs release in the 0.01 mg/LGO-exposure group is lower than other groups. However, when the GO-exposure concentration was 10 mg/L, as demonstrated in **Fig**. 5B, the level of ROS in algal cell increased sharply. The level of ROS in the algal cells increased sharply with increasing GO in the media. The increased ROS and occurrence of cell rupture explain the decreased nutrients removal and significantly increased ($p < 0.05$) extracellular MCs in the 10 mg/L GO-exposure group. The TEM images in **Fig**. 5A showed obscure boundaries of the cytomembranes, indicating that severe peroxidation damage and plasmolysis of the algal cells occurred, and a large number of cells were ruptured in the high GO concentration treatments (the red circle in **Fig**. 2A). Thereupon, lots of intracellular MCs were released, and the percentage of extracellular MCs release was increased significantly ($p<0.05$).

Furthermore, as shown in **Fig**. 3A and **Fig**. 3B, the value of F_v/F_m and ETR_{max} of *M. aeruginosa* cells were the highest among all groups during the GO-exposure was 0.01 mg/L. The F_v/F_m value reflects the potential maximum photosynthetic capacity of algal cells (Joonas et al. 2019), and the ETR_{max} value reflects the maximum transmission rate of photons in photosynthesis of *M. aeruginosa* (Lee et al. 2019). The higher F_v/F_m and ETR_{max} values would indicate the better photosynthetic performance (Cruces et al. 2021), and F_v/F_m value of normal growth of algae is about 0.7-0.8 (Zheng et al. 2020). The highest F_v/F_m value is 1.1 in group of GO-exposure at concentration of 0.01 mg/L. Therefore, the photosynthetic performance was stimulated by GO-exposure at concentration of 0.01 mg/L. In contrast, the F_v/F_m and ETR_{max} values in GO-exposure at concentration of 10 mg/L are the lowest among all groups. From another perspective, the higher the F_v/F_m and ETR_{max} values would indicate the less stressed conditions in growth environment of *M. aeruginosa*. The lower the F_v/F_m and ETR_{max} values would indicate the more stressed conditions in growth environment and the worse photosynthetic performance

(Sanz-Martín et al. 2019). Photosynthetic performance, the growth rate in *M. aeruginosa* increased under 0.01 mg/L GO-exposure and decreased under 10 mg/L GO-exposure (**Fig**. 6C). These results suggested that slight GO-exposure enhanced the photosynthetic activity, growth rate, and MCs production of *M. aeruginosa* at environmentally relevant concentrations. it could reasonably be inferred that the GO pollution at environmentally relevant concentrations would aggravate the ecological hazard of *M. aeruginosa* (Gao et al. 2019).

3.4 Analysis of interactions from metabolomic aspects

The metabolic pattern of *M. aeruginosa* under GO-exposures of 0.01 mg/L and 10 mg/L were compared with the control without GO-exposure. The GO-exposures at concentration of 0.01 mg/L and 10 mg/L were close to the low and high contamination levels of GO in aquatic environments, respectively (Zhang et al. 2020a). The metabolic profiling of *M. aeruginosa* in 0.01 and 10 mg/L GO-exposure groups are distinct (**Fig**. 7A), indicating that the metabolites in these two groups are significantly different ($p < 0.05$). A total of 64 differential metabolites were screened (**Fig**. 7B), while the relative abundance of differential metabolites (**Fig**. 7C) and significantly different metabolic pathways ($p < 0.05$) in the GO-exposed groups were analyzed (**Fig**. 8).

After 96 h of exposure to 0.01 mg/L of GO, 56 metabolites were upregulated while 8 metabolites were down-regulated (**Table** 1). The identified metabolites were involved in 4 main physiological processes according to significant enriched pathways ($p < 0.05$), including photosynthetic metabolism, glycometabolism, amino acid metabolism, and lipid metabolism. Much more metabolites were up-regulated instead of down-regulated, indicating that most physiological activities in *M. aeruginosa* were stimulated at the presence of 0.01 mg/L GO. In contrast, after 96 h of GO-exposure at concentration of 10 mg/L, 47 metabolites were up-regulated while 17 metabolites were down-regulated. More metabolites were down-regulated as compared with the 0.01 mg/L GO treatment, suggesting that the physiological activities were motivated to initiate the defensive mechanism against GO stress in the 10 mg/L GO treatment (Zhang et al. 2019). The result of enrichment analysis of KEGG pathway demonstrated that carbon fixation in photosynthetic process, valine, leucine and isoleucine biosynthesis, and galactose metabolism were significantly

289 enriched ($p<0.05$) in *M. aeruginosa* exposed to GO at concentration of 0.01 mg/L.

290 The metabolic network map reflects the important interactions between the altered metabolic
291 pathways (**Fig**. 8). Notably, in 0.01 mg/L GO-exposure group, an increase in amino acid metabolism
292 including increase in L-threonine, L-valine, L-alanine, and L-proline, was observed. These findings
293 are in accordance with previous studies where an increase in amino acid turnover in stimulated algal
294 cells by low concentration of GO was reported (Ouyang et al. 2020). The other important metabolic
295 pathway found to be altered in *M. aeruginosa* in 0.01 GO-exposure group was nucleotide
296 metabolism, including increase of uracil and hypoxanthine. Proliferating algal cells of *M.*
297 *aeruginosa* stimulated by GO often demand for nucleotides for the synthesis of cellular materials,
298 which is fulfilled by purines and pyrimidines. Increases in nucleotides indicate that they are needed
299 for cell proliferation (Zhang et al. 2020b). Additionally, glycometabolism and fatty acid
300 metabolism were indicated to be alerted in *M. aeruginosa* at GO-exposure of 0.01 mg/L.
301 Specifically, increased levels of carbohydrates and numerous unsaturated fatty acids including
302 D-glucose, galacturonate, linoleic acid, glutaric, and tetradecanoic acid were observed. The increase
303 of glycometabolism indicates the vigorous growth of algal cell (Zhang et al. 2018), and unsaturated
304 fatty acid will promote the photosynthetic performance of algal cells (Anto et al. 2020).

305 Moreover, the reticular correlativity between differential metabolites and other results including
306 TN, NH_3-N, PO_4^{3-}-P, COD, *mcyA-J* gene copies, MCs production, ARGs (*sul1*, *sul2*, *tetW*, *tetM*),
307 F_v/F_m, ETR_{max}, and growth rate were calculated. Highly interconnected metabolites with high
308 degrees play key roles in the interaction of *M. aeruginosa* and GO. According to the correlativity
309 analysis between metabolites and other pollutants and factors (*sul1*, *sul2*, *tetM*, *tetW*, *mcyA-J*, MCs
310 production, NH_3-N, TN, PO_4^{3-}-P, COD, F_v/F_m, ETR_{max}, growth rate, ROS, and 16S rRNA) as shown
311 in **Fig**. 9. Moreover, it demonstrated that there were 23 pairs of positive correlations between the
312 intracellular differential metabolites of *M. aeruginosa* and the abundances of *sul1*, *sul2*, *tetM*, and
313 *tetW* with different GO concentrations. The metabolites that related ARGs abundance were mainly
314 amino acids. The metabolites that related *mcyA-J* expression were mainly amino acids and small
315 molecule acids. There were 40 pairs of positive correlations between these metabolites and *mcyA-J*.
316 Furthermore, there were 28 pairs of positive correlations between the abundance of *sul1*, *sul2*, *tetM*,

317 *tetW* and *mcyA-J* expression. The impacts and interactions were complicated of abundance of ARGs,
318 *mcyA-J* expression, MCs production, photosynthesis performance of *M. aeruginosa*, intracellular
319 ROS levels, ultrastructure, and GO. Simultaneously, there is also a close correlation among various
320 different metabolites in *M aeruginosa* (Kim et al. 2020).

321 Some chemical substances such as antibiotic contaminants and organic pollutant have been
322 manifest to have toxic stimulant hormesis effects on algae at a certain concentration (Liu et al.
323 2020). Nanomaterials are also reported to have a hormesis effect on many kinds of algal cells
324 (Agathokleous et al. 2019). The phenomenon of hormesis effect was observed in the *M.*
325 *aeruginosa* in GO-exposure in the present study. Photosynthesis is the basis of a cell growth of *M.*
326 *aeruginosa*, photosynthetic performance was promoted by GO-exposure at 0.01 mg/L (Wang et al.
327 2020b). The GO stimulated the growth rate, and then promoted the production of MCs in *M.*
328 *aeruginosa* (Yu et al. 2019).

329 Particularly, the gene copies of microcystin synthetase (*mcyA-J*) increased. It was reasonable to
330 conclude that the increased genetic expression of microcystin synthetase had resulted in the
331 increased production of MCs. In contrast, the expression of *mcyA-J* was inhibited in the 10 mg/L
332 GO- exposed group, and consequently, MCs production decreased. The results suggested that the
333 MCs synthetic process is stimulated by low and inhibited by high concentration of GO.

334 The ARGs and *mcyA-J* were significantly related with photosynthetic metabolites including
335 phytol (an essential component of chlorophyll) and 3-6-anhydro-D-glucose (photosynthetic carbon
336 fixes important metabolites) (Zhang et al. 2018). Moreover, some studies have demonstrated that
337 microcystin synthetase genes (*mcyA-J*) and MCs production was a kind of physiological response
338 to environmental stressed factors (Li et al. 2019). These results confirmed that the role of MCs
339 production and synthesis in responsive process to GO-exposure at environmental concentration (Li
340 et al. 2019).

341 The *M. aeruginosa* released more MCs in the 10 mg/L GO-exposure group than in the control
342 and the 0.01 mg/L GO treatment. The increased ROS level and membranolysis (**Fig**. 5) may
343 facilitate the export of intracellular MCs (Li et al. 2019). The cells rupturing induced by
344 GO-exposure might be an important explanation for the MCs release by *M. aeruginosa* (Li et al.

2020). With increased intracellular MCs production and *sul1*, *sul2*, *tetM*, *tetW* abundance at low concentration of GO and increased release of MCs at high concentration of GO, the hazards of *M. aeruginosa* and ARGs would be exacerbated by GO in the aquatic environment (Bandara et al. 2019). It suggested that the harm of GO by regulating the ARGs abundance, microcystin synthetase genes, and MCs production has already become an ecological problem.

During the GO-exposure period of 96 h, impacts and interactions of ARGs, microcystin synthetase genes, MCs production, photosynthesis were initiated. The relative abundance of carbohydrates related to the carbon fixation pathway in photosynthetic process in *M. aeruginosa* increased significantly ($p < 0.05$) in GO-exposure at concentration of 0.01 mg/L. Simultaneously, the expression of *mcyA-J* in *M. aeruginosa* and *sul1*, *sul2*, *tetM*, *tet W* in synthetic wastewater increased significantly ($p < 0.05$), resulting in the increase of intracellular MCs production and ARGs spread. The microcystin synthetase gene cluster of *mcyA-J* can regulate the ABC transporters (control the transportation and exchange of nutrients between extracellular and intracellular) (Han et al. 2019, Pearson et al. 2020). The result of KEGG pathway enrichment analysis suggested that the pathway of ABC transporters was significantly enriched, and the metabolites (valine, maltotriose, D-glucose, D-maltose, threonine, alanine, proline) which matched in the transporter pathway were up-regulated. It means that more extracellular nutrients (such as NH_3-N) and ARGs plasmid of *sul1*, *sul2*, *tetM*, tetW in synthetic wastewater will be transported into *M. aeruginosa* for cell growth, MCs synthesis and spread of ARGs (Yu et al. 2019). When the concentration of GO−exposure increased to 10 mg/L, cytoderm rupture occurred and large amounts of intracellular MCs was released. It indicated that hormesis mechanism would be triggered in *M. aeruginosa* and ARGs abundance when the GO presents. The presence of GO at finite concentration in aquatic environment can aggravate the harm of *M. aeruginosa* and spread of ARGs (Duan et al. 2020, Huang et al. 2020).

4. Conclusions

Mutual impacts and interactions of antibiotic resistance genes, microcystin synthetase genes,

graphene oxide, and *M. aeruginosa* in synthetic wastewater were investigated in the present study. There was significant correlation between the abundance of ARGs (*sul1*, *sul2*, *tetM*, *tetW*) and *mcyA-J* expression when the GO concentration was 0.01 mg/L. GO has a hormesis effect on *M. aeruginosa*, ARGs abundance, and *mcyA-J* expression. At low concentration of 0.01 mg/L, GO would stimulate the photosynthesis and growth of *M. aeruginosa*, while at high concentration of 10 mg/L, GO would induce cell rupture and MCs release of *M. aeruginosa*. The GO in aquatic environment would aggravate the ecological hazard of *M. aeruginosa* by promoting its growth, *mcyA-J* expression, MCs production, and ARGs abundance.

Acknowledgments

This work was financially sponsored by Shanghai Sailing Program (20YF1447700) and National Natural Science Foundation of China (32001201).

Funding Information

(1) Shanghai Sailing Program

Award Number: 20YF1447700 | Recipient: Xiyan Ji

(2) National Natural Science Foundation of China

Award Number: 32001201 | Recipient: Xiyan Ji

Ethical Approval

This research does not involve ethical issues.

Consent to Participate

This research does not involve ethical issues.

Consent to Publish

All authors confirm that this paper has not been published before in any form.

Authors Contributions

Xiyan Ji: Conceptualization, Methodology, Supervision, Funding acquisition

Meifang Hou: Supervision, Conceptualization, Review & Editing

Shichao Wu: Validation, Formal analysis, Investigation, Data Curation, Writing - Original Draft

Xin Li: Resources, Data Curation, Formal analysis

Jing Ye: Review & Editing

Wenwu Xu: Project administration

Rui Wang: Visualization

Competing Interests

The authors declare that they have no known competing financial interests or personal relationships that could have appeared to influence the work reported in this paper.

Availability of data and materials

The datasets used or analyzed during the current study are available from the corresponding author on reasonable request.

References

Agathokleous E, Feng Z, Iavicoli I, Calabrese EJJEi (2019): The two faces of nanomaterials: A quantification of hormesis in algae and plants. 131, 105044

Ajayan K, Harilal C, Gani PJAR (2019): Performance of reflector coated LED Bio-box on the

411 augmentation of growth and lipid production in aerophytic trebouxiophyceaen algae
412 Coccomyxa sp. 38, 101401
413 Anto S, Mukherjee SS, Muthappa R, Mathimani T, Deviram G, Kumar SS, Verma TN, Pugazhendhi AJC
414 (2020): Algae as green energy reserve: Technological outlook on biofuel production. 242,
415 125079
416 Aphale A, Chattopadhyay A, Mahakalakar K, Patra PJJon, nanotechnology (2015): Synthesis and
417 electrochemical analysis of algae cellulose-polypyrrole-graphene nanocomposite for
418 supercapacitor electrode. 15, 6225-6229
419 Avant B, Bouchard D, Chang X, Hsieh H-S, Acrey B, Han Y, Spear J, Zepp R, Knightes CDJN (2019):
420 Environmental fate of multiwalled carbon nanotubes and graphene oxide across different
421 aquatic ecosystems. 13, 1-12
422 Bandara PC, Perez JVD, Nadres ET, Nannapaneni RG, Krakowiak KJ, Rodrigues DFJAAPM (2019):
423 Graphene oxide nanocomposite hydrogel beads for removal of selenium in contaminated water.
424 1, 2668-2679
425 Chen L, Chen J, Zhang X, Xie PJJohm (2016): A review of reproductive toxicity of microcystins. 301,
426 381-399
427 Conley DJ, Paerl HW, Howarth RW, Boesch DF, Seitzinger SP, Karl E KE, Lancelot C, Gene E GEJS
428 (2009): Controlling eutrophication: nitrogen and phosphorus. 123, 1014-1015
429 Cruces E, Barrios AC, Cahue YP, Januszewski B, Gilbertson LM, Perreault FJC (2021): Similar toxicity
430 mechanisms between graphene oxide and oxidized multi-walled carbon nanotubes in
431 Microcystis aeruginosa. 265, 129137
432 Duan Y, Guo X, Yang J, Zhang M, Li YJRSos (2020): Nutrients recycle and the growth of Scenedesmus
433 obliquus in synthetic wastewater under different sodium carbonate concentrations. 7, 191214
434 Elser JJ, Bracken ME, Cleland EE, Gruner DS, Harpole WS, Hillebrand H, Ngai JT, Seabloom EW,
435 Shurin JB, Smith JEJEl (2007): Global analysis of nitrogen and phosphorus limitation of
436 primary producers in freshwater, marine and terrestrial ecosystems. 10, 1135-1142
437 Fan G, Ning R, Yan Z, Luo J, Du B, Zhan J, Liu L, Zhang JJJoHM (2021): Double photoelectron-transfer
438 mechanism in Ag− AgCl/WO3/g-C3N4 photocatalyst with enhanced visible-light
439 photocatalytic activity for trimethoprim degradation. 403, 123964
440 Gao M, Yang Y, Song ZJE, safety e (2019): Effects of graphene oxide on cadmium uptake and

photosynthesis performance in wheat seedlings. 173, 165-173

Grasso G, Zane D, Dragone RJN (2020): Microbial nanotechnology: Challenges and prospects for green biocatalytic synthesis of nanoscale materials for sensoristic and biomedical applications. 10, 11

Guo J, Ma Z, Peng J, Mo J, Li Q, Guo J, Yang FJJoHM (2021): Transcriptomic analysis of Raphidocelis subcapitata exposed to erythromycin: The role of DNA replication in hormesis and growth inhibition. 402, 123512

Han T, Liang Y, Wu Z, Zhang L, Liu Z, Li Q, Chen X, Guo W, Jiang L, Pan FJJohm (2019): Effects of tetracycline on growth, oxidative stress response, and metabolite pattern of ryegrass. 380, 120885

Huang F, Pan L, He Z, Zhang M, Zhang MJSoTTE (2020): Identification, interactions, nitrogen removal pathways and performances of culturable heterotrophic nitrification-aerobic denitrification bacteria from mariculture water by using cell culture and metagenomics. 732, 139268

Jiang Y, Liu Y, Zhang JJEP (2020): Antibiotic contaminants reduced the treatment efficiency of UV-C on Microcystis aeruginosa through hormesis. 261, 114193

Jiang Y, Liu Y, Zhang JJJoHM (2021): Mechanisms for the stimulatory effects of a five-component mixture of antibiotics in Microcystis aeruginosa at transcriptomic and proteomic levels. 406, 124722

Joonas E, Aruoja V, Olli K, Kahru AJSotte (2019): Environmental safety data on CuO and TiO2 nanoparticles for multiple algal species in natural water: filling the data gaps for risk assessment. 647, 973-980

Kim M, Lee J, Yang D, Park HY, Park WJEP (2020): Seasonal dynamics of the bacterial communities associated with cyanobacterial blooms in the Han River. 266, 115198

Komijani M, Shamabadi NS, Shahin K, Eghbalpour F, Tahsili MR, Bahram MJEP (2021): Heavy metal pollution promotes antibiotic resistance potential in the aquatic environment. 274, 116569

Lee H, Brown MT, Choi S, Pandey LK, De Saeger J, Shin K, Kim JK, Depuydt S, Han T, Park JJJohm (2019): Reappraisal of the toxicity test method using the green alga Ulva pertusa Kjellman (Chlorophyta). 369, 763-769

Lee J, Choi J, Fatka M, Swanner E, Ikuma K, Liang X, Leung T, Howe AJWr (2020): Improved detection of mcyA genes and their phylogenetic origins in harmful algal blooms. 176, 115730

Li S, Tao Y, Zhan X-M, Dao G-H, Hu H-YJSoTTE (2020): UV-C irradiation for harmful algal blooms control: A literature review on effectiveness, mechanisms, influencing factors and facilities. 723, 137986

Li X, Li J, Meng F, Yao LJE, safety e (2019): Hepatotoxicity and immunotoxicity of MC-LR on silver carp. 169, 28-32

Liu X, Yan B, Li Y, Ma X, Jiao W, Shi K, Zhang T, Chen S, He Y, Liang X-JJAn (2020): Graphene oxide-grafted magnetic nanorings mediated magnetothermodynamic therapy favoring reactive oxygen species-related immune response for enhanced antitumor efficacy. 14, 1936-1950

Lu J, Struewing I, Wymer L, Tettenhorst DR, Shoemaker J, Allen JJWr (2020a): Use of qPCR and RT-qPCR for monitoring variations of microcystin producers and as an early warning system to predict toxin production in an Ohio inland lake. 170, 115262

Lu N, Ling L, Guan T, Wang L, Wang D, Zhou J, Ruan T, Shen X, Li X, Sun YJT (2020b): Broad-specificity ELISA with a heterogeneous strategy for sensitive detection of microcystins and nodularin. 175, 44-48

Ma X, Zhou W, Fu Z, Cheng Y, Min M, Liu Y, Zhang Y, Chen P, Ruan RJBt (2014): Effect of wastewater-borne bacteria on algal growth and nutrients removal in wastewater-based algae cultivation system. 167, 8-13

McLellan NL, Manderville RAJTr (2017): Toxic mechanisms of microcystins in mammals. 6, 391-405

Monteil C, Bar N, Moreau B, Retoux R, Bee A, Talbot D, Villemin DJP, Characterization PS (2014): Phosphonated Polyethylenimine-Coated Nanoparticles: Size-and Zeta-Potential-Adjustable Nanomaterials. 31, 219-227

Ouyang S, Zhou Q, Zeng H, Wang Y, Hu XJEs, technology (2020): Natural Nanocolloids Mediate the Phytotoxicity of Graphene Oxide. 54, 4865-4875

Pan S-D, Chen X-H, Li X-P, Cai M-Q, Shen H-Y, Zhao Y-G, Jin M-CJJoMCA (2015): In situ controllable synthesis of graphene oxide-based ternary magnetic molecularly imprinted polymer hybrid for efficient enrichment and detection of eight microcystins. 3, 23042-23052

Pearson LA, Crosbie ND, Neilan BAJM, Research F (2020): Distribution and conservation of known secondary metabolite biosynthesis gene clusters in the genomes of geographically diverse Microcystis aeruginosa strains. 71, 701-716

Pinheiro C, Azevedo J, Campos A, Vasconcelos V, Loureiro SJE (2016): The interactive effects of

microcystin-LR and cylindrospermopsin on the growth rate of the freshwater algae Chlorella vulgaris. 25, 745-758

Poudyal D, Rosenqvist E, Ottosen C-OJFpb (2019): Phenotyping from lab to field–tomato lines screened for heat stress using Fv/Fm maintain high fruit yield during thermal stress in the field. 46, 44-55

Rincon SM, Urrego NF, Avila KJ, Romero HM, Beyenal HJAR (2019): Photosynthetic activity assessment in mixotrophically cultured Chlorella vulgaris biofilms at various developmental stages. 38, 101408

Rzymski P, Klimaszyk P, Jurczak T, Poniedziałek BJFiM (2020): Oxidative stress, programmed cell death and microcystin release in Microcystis aeruginosa in response to Daphnia grazers. 11

Sanz-Martín M, Hendriks IE, Carstensen J, Marbà N, Krause-Jensen D, Sejr MK, Duarte CMJAB (2019): Continuous photoperiod of the Artic summer stimulates the photosynthetic response of some marine macrophytes. 158, 103126

Soares C, Pereira R, Martins M, Tamagnini P, Serôdio J, Moutinho-Pereira J, Cunha A, Fidalgo FJJoHM (2020): Glyphosate-dependent effects on photosynthesis of Solanum lycopersicum L.—An ecophysiological, ultrastructural and molecular approach. 398, 122871

Sola AJN (2020): Abuse of antibiotics in perinatology: negative impact for health and the economy. 21, e559-e570

Sun J, Bu L, Deng L, Shi Z, Zhou SJCEJ (2018): Removal of Microcystis aeruginosa by UV/chlorine process: Inactivation mechanism and microcystins degradation. 349, 408-415

Sun W, Qian X, Gu J, Wang X-J, Zhang L, Guo A-YJBt (2017): Mechanisms and effects of arsanilic acid on antibiotic resistance genes and microbial communities during pig manure digestion. 234, 217-223

Sun Y, Cao N, Duan C, Wang Q, Ding C, Wang JJJoHM (2021): Selection of antibiotic resistance genes on biodegradable and non-biodegradable microplastics. 409, 124979

Wang C, Yang Y, Hou J, Wang P, Miao L, Wang X, Guo LJAR (2020a): Optimization of cyanobacterial harvesting and extracellular organic matter removal utilizing magnetic nanoparticles and response surface methodology: A comparative study. 45, 101756

Wang H, Jin M, Mao W, Chen C, Fu L, Li Z, Du S, Liu HJSoTTE (2020b): Photosynthetic toxicity of non-steroidal anti-inflammatory drugs (NSAIDs) on green algae Scenedesmus obliquus. 707,

136176

Weckwerth W, Wenzel K, Fiehn OJP (2004): Process for the integrated extraction, identification and quantification of metabolites, proteins and RNA to reveal their co-regulation in biochemical networks. 4, 78-83

Wei J, Xie X, Huang F, Xiang L, Wang Y, Han T, Massey IY, Liang G, Pu Y, Yang FJEp (2020): Simultaneous Microcystis algicidal and microcystin synthesis inhibition by a red pigment prodigiosin. 256, 113444

Wu D-L, Zhang M, He L-X, Zou H-Y, Liu Y-S, Li B-B, Yang Y-Y, Liu C, He L-Y, Ying G-GJSoTTE (2020a): Contamination profile of antibiotic resistance genes in ground water in comparison with surface water. 715, 136975

Wu X, Wu H, Gu X, Zhang R, Sheng Q, Ye JJEP (2020b): Effect of the immobilized microcystin-LR-degrading enzyme MlrA on nodularin degradation and its immunotoxicity study. 258, 113653

Xu S, Liu Y, Zhang J, Gao BJC (2021): Proteomic mechanisms for the combined stimulatory effects of glyphosate and antibiotic contaminants on Microcystis aeruginosa. 267, 129244

Yang Z, Kong F, Shi X, Yu Y, Zhang MJJoHM (2015): Effects of UV-B radiation on microcystin production of a toxic strain of Microcystis aeruginosa and its competitiveness against a non-toxic strain. 283, 447-453

Yang Z, Hao X, Chen S, Ma Z, Wang W, Wang C, Yue L, Sun H, Shao Q, Murugadoss VJJoc, science i (2019): Long-term antibacterial stable reduced graphene oxide nanocomposites loaded with cuprous oxide nanoparticles. 533, 13-23

Yin J, Fan W, Du J, Feng W, Dong Z, Liu Y, Zhou TJEP (2020): The toxicity of graphene oxide affected by algal physiological characteristics: A comparative study in cyanobacterial, green algae, diatom. 260, 113847

Yu S, Li C, Xu C, Effiong K, Xiao XJE, safety e (2019): Understanding the inhibitory mechanism of antialgal allelochemical flavonoids from genetic variations: photosynthesis, toxin synthesis and nutrient utility. 177, 18-24

Zhang H, Meng G, Mao F, Li W, He Y, Gin KY-H, Ong CNJJohm (2019): Use of an integrated metabolomics platform for mechanistic investigations of three commonly used algaecides on cyanobacterium, Microcystis aeruginosa. 367, 120-127

561 Zhang M, Wang X, Tao J, Li S, Hao S, Zhu X, Hong YJE, safety e (2018): PAHs would alter
562 cyanobacterial blooms by affecting the microcystin production and physiological characteristics
563 of Microcystis aeruginosa. 157, 134-142
564 Zhang Q, Hou Q, Huang G, Fan QJES, Research P (2020a): Removal of heavy metals in aquatic
565 environment by graphene oxide composites: a review. 27, 190-209
566 Zhang X, Hu C, Sun X, Zang X, Zhang X, Fang T, Xu NJA (2020b): Comparative transcriptome analysis
567 reveals chitooligosaccharides-induced stress tolerance of Gracilariopsis lemaneiformis under
568 high temperature stress. 519, 734876
569 Zhao P, Liu S, Huang W, He L, Li J, Zhou J, Zhou JJC (2020a): Influence of eugenol on algal growth, cell
570 physiology of cyanobacteria Microcystis aeruginosa and its interaction with signaling
571 molecules. 255, 126935
572 Zhao Y, Liu Y, Zhang X, Liao WJC (2020b): Environmental transformation of graphene oxide in the
573 aquatic environment. 127885
574 Zheng L, Steppe K, Van Labeke MCJPp (2020): Spectral quality of monochromatic LED affects
575 photosynthetic acclimation to high-intensity sunlight of Chrysanthemum and Spathiphyllum.
576 169, 10-26
577 Zhu G, Cui X, Zhang Y, Chen S, Dong M, Liu H, Shao Q, Ding T, Wu S, Guo ZJP (2019): Poly (vinyl
578 butyral)/graphene oxide/poly (methylhydrosiloxane) nanocomposite coating for improved
579 aluminum alloy anticorrosion. 172, 415-422
580

Figures

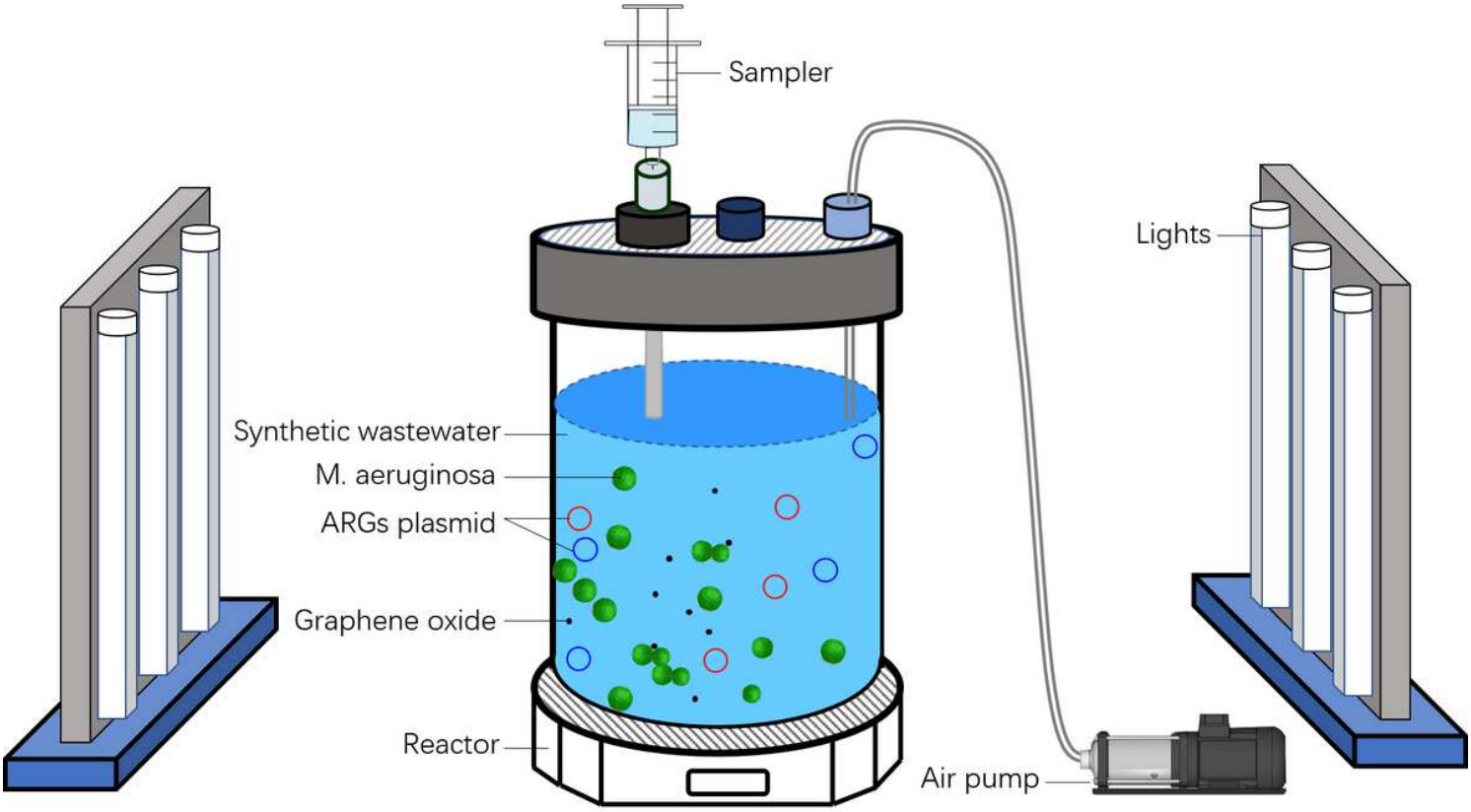

Figure 1

Schematic diagram of experimental set-up

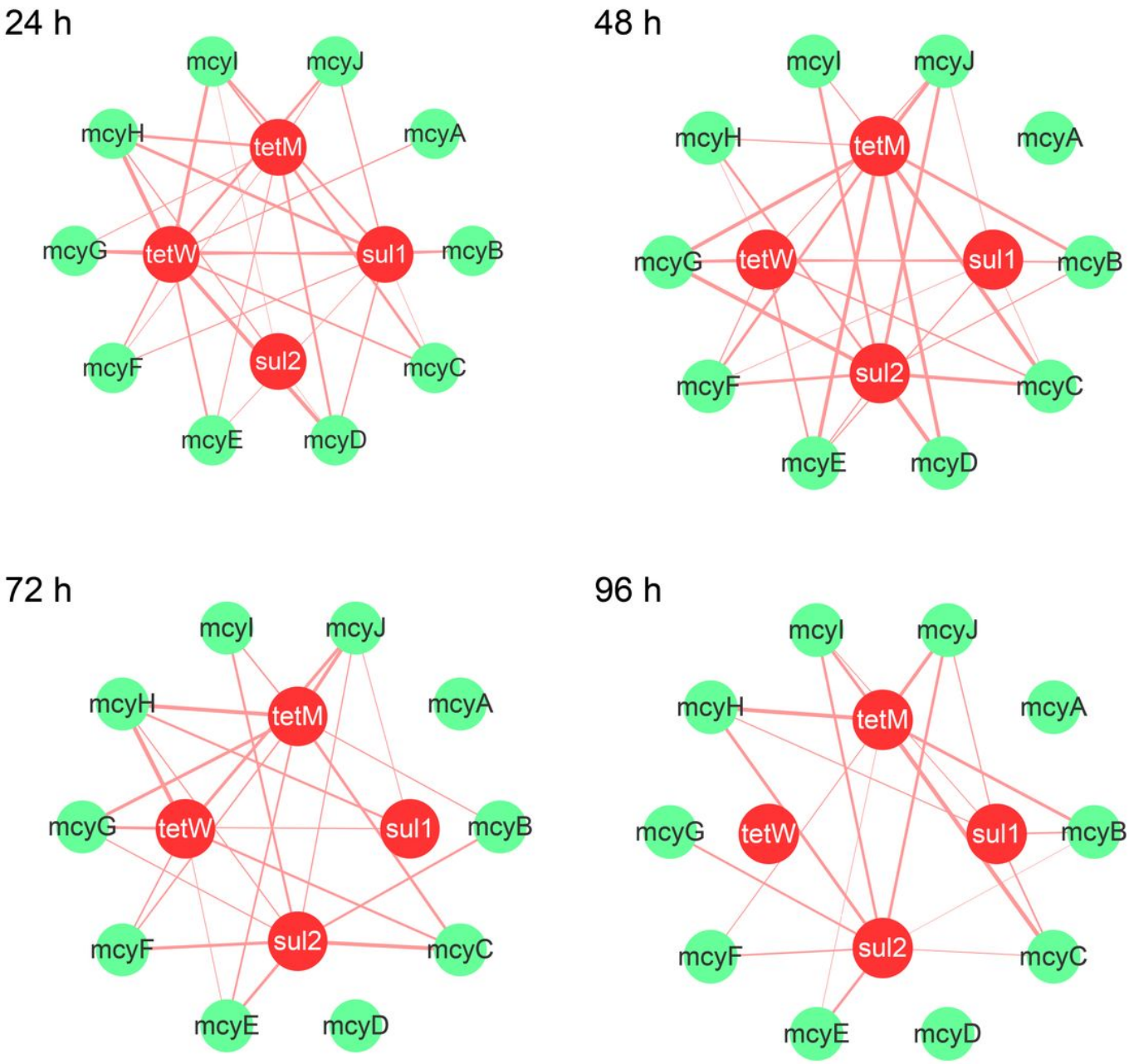

Figure 2

Pearson correlation analysis between abudances of sul1, sul2, tetM, tetW and mcyA-J expressions

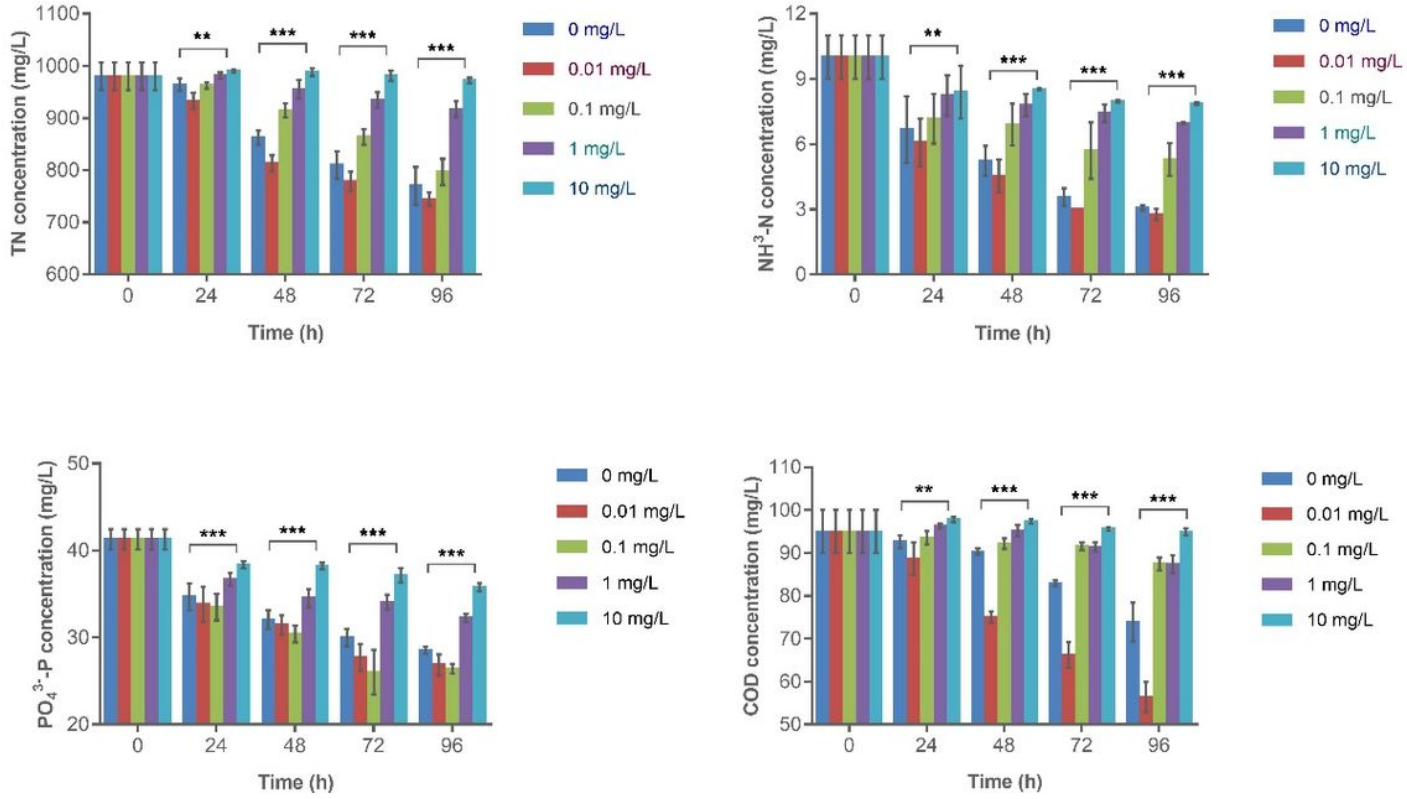

Figure 3

Changes in TN, NH3-N, PO43-P, and COD concentrations during the 96-h incubation of M. aeruginosa in BG11 medium with 0, 0.01, 0.1, 1, and 10 mg/L graphene oxide (GO)

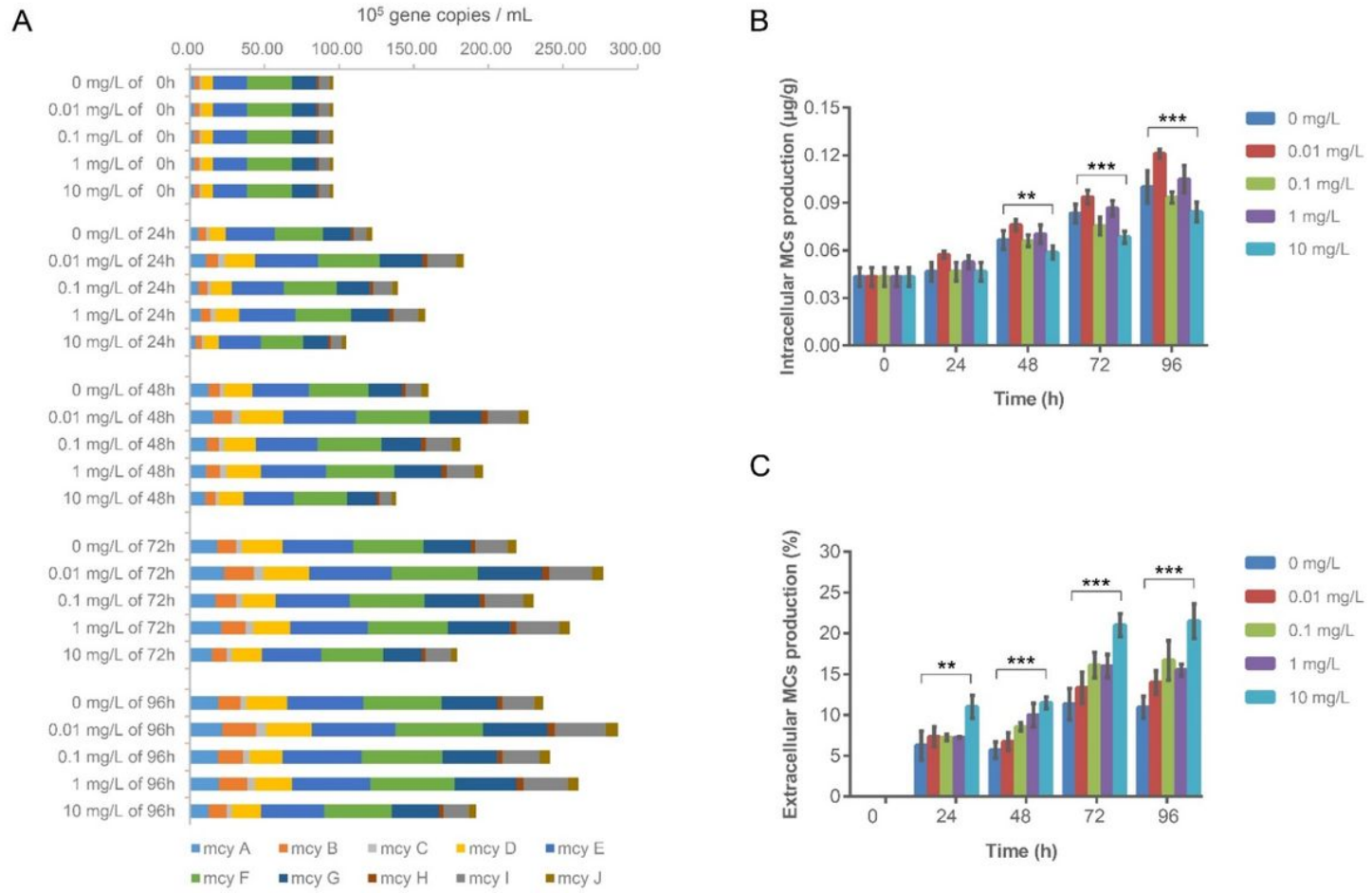

Figure 4

A: The expression of microcystis synthase gene cluster (mcy A-J) in M. aeruginosa in 0.01, 0.1, 1, 10 mg/L GO-exposure groups and control group; B: The intracellular MCs production in M. aeruginosa in 0.01, 0.1, 1, 10 mg/L GO-exposure groups and control group; C: The percentage of extracellular MCs production in M. aeruginosa in 0.01, 0.1, 1, 10 mg/L GO-exposure groups and control group.

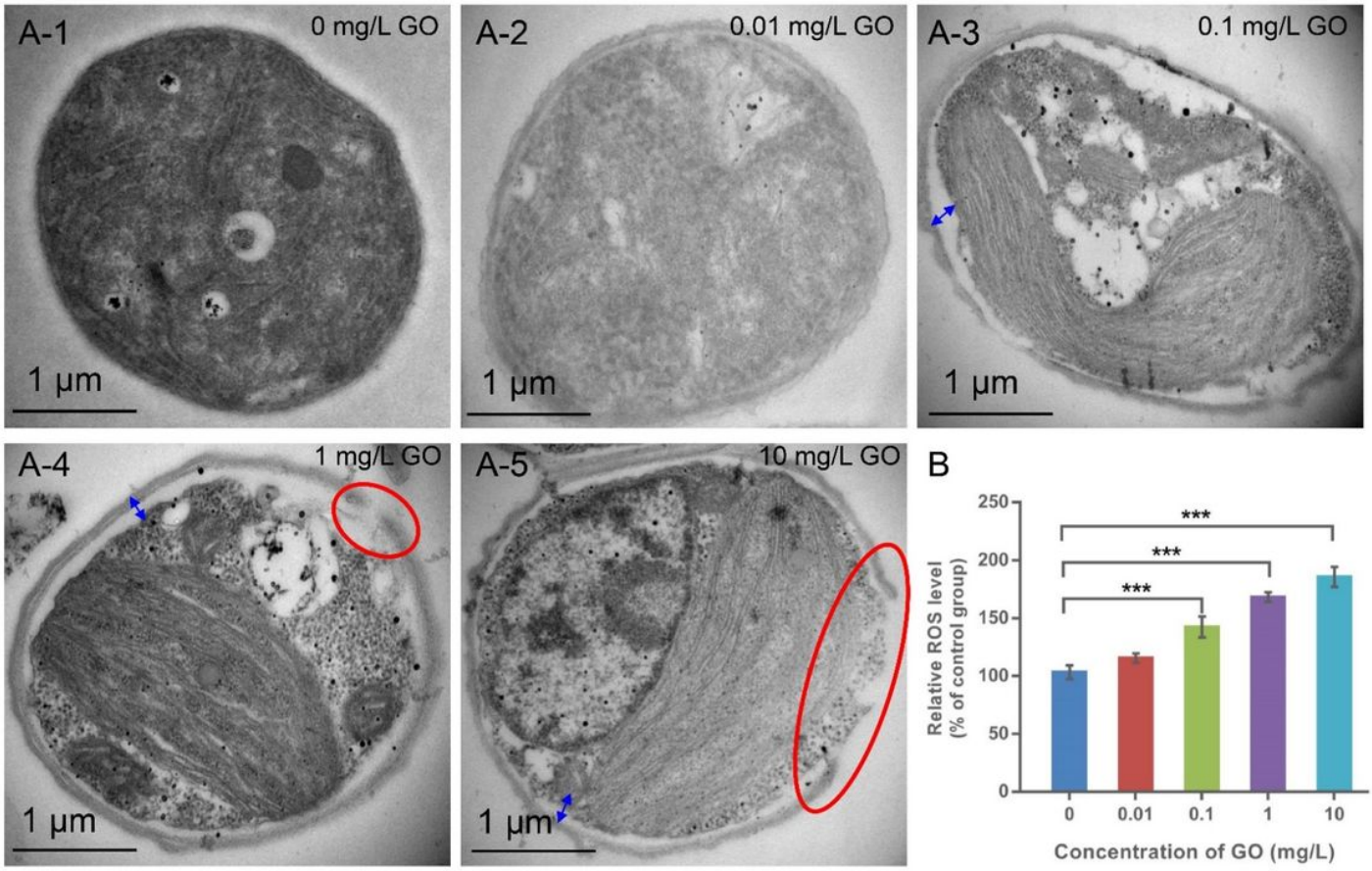

Figure 5

The TEM images and ROS levels of M. aeruginosa in 0.01, 0.1, 1, 10 mg/L GO-exposure groups and control group. A1-A5: ultrastructure of the M. aeruginosa. double-headed arrows denote plasmolysis of M. aeruginosa, red circles denote breakages of M. aeruginosa. B: ROS levels of M. aeruginosa in all groups.

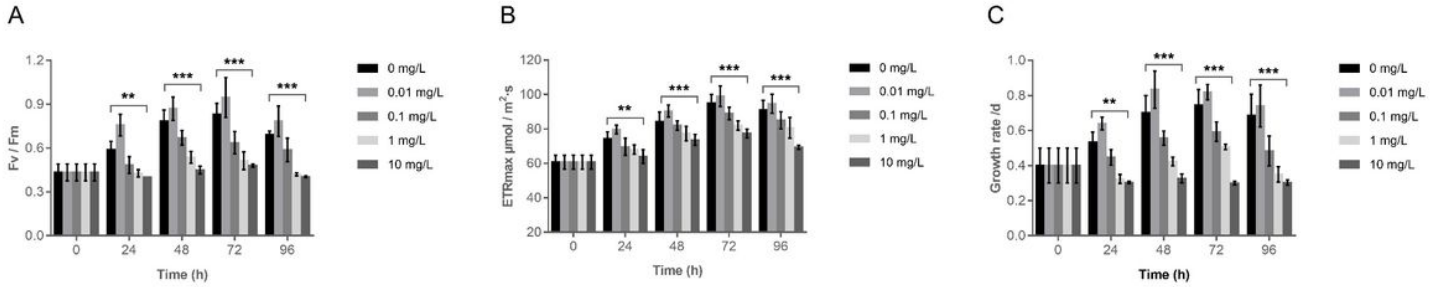

Figure 6

The Fv/Fm, ETRmax, and growth rate of M. aeruginosa in 0, 0.01, 0.1, 1, 10 mg/L GO-exposure groups and control group. A: Fv/Fm of the M. aeruginosa in all groups, B: ETRmax of the M. aeruginosa in all groups, C: growth rate of the M. aeruginosa in all groups.

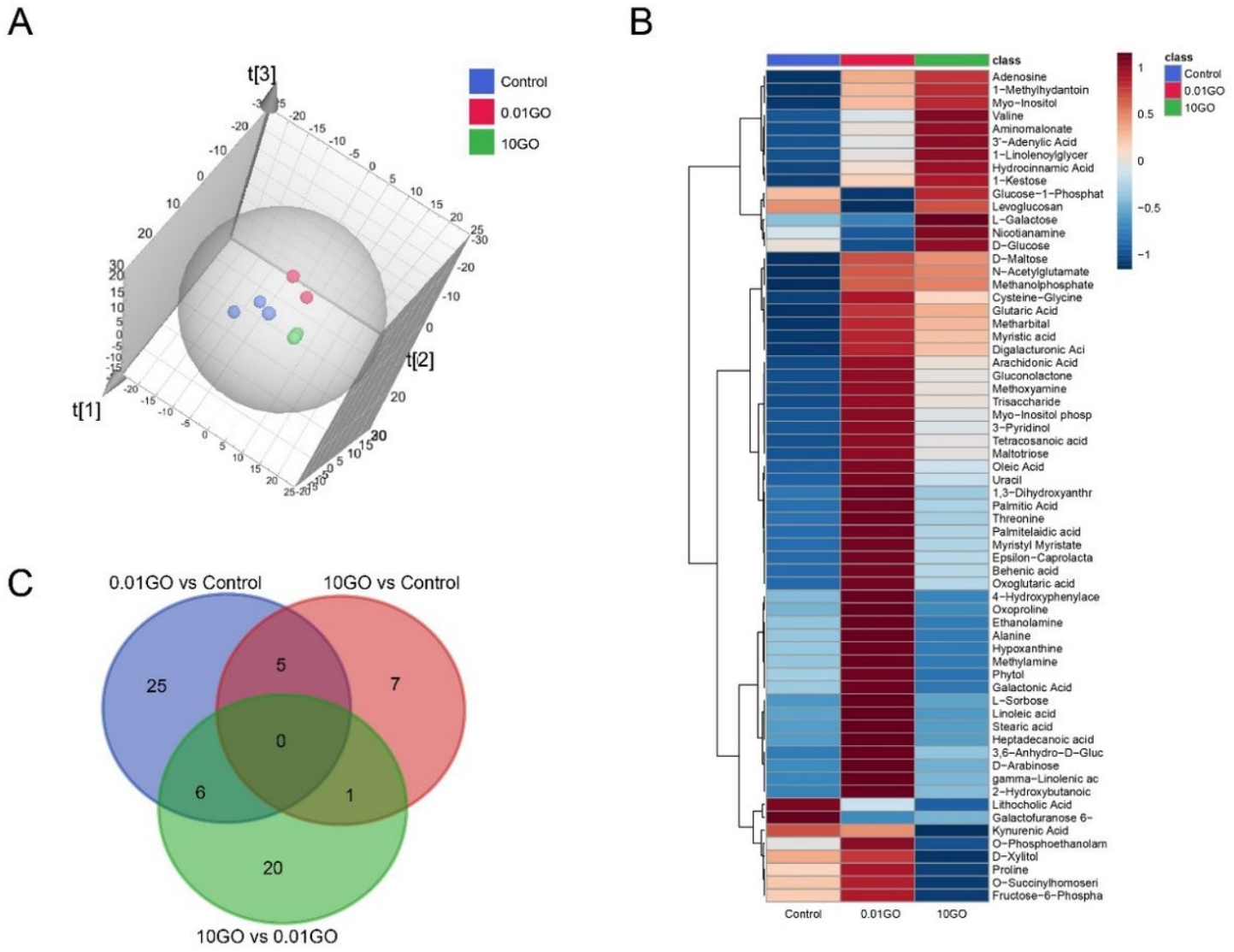

Figure 7

The metabolic analysis of M. aeruginosa in different concentration of GO-exposure. A: PCA analysis, B: metabolite heat map of control group, 0.01 mg/L GO-exposure, 10 mg/L GO-exposure. C: venn diagram of the differential metabolites.

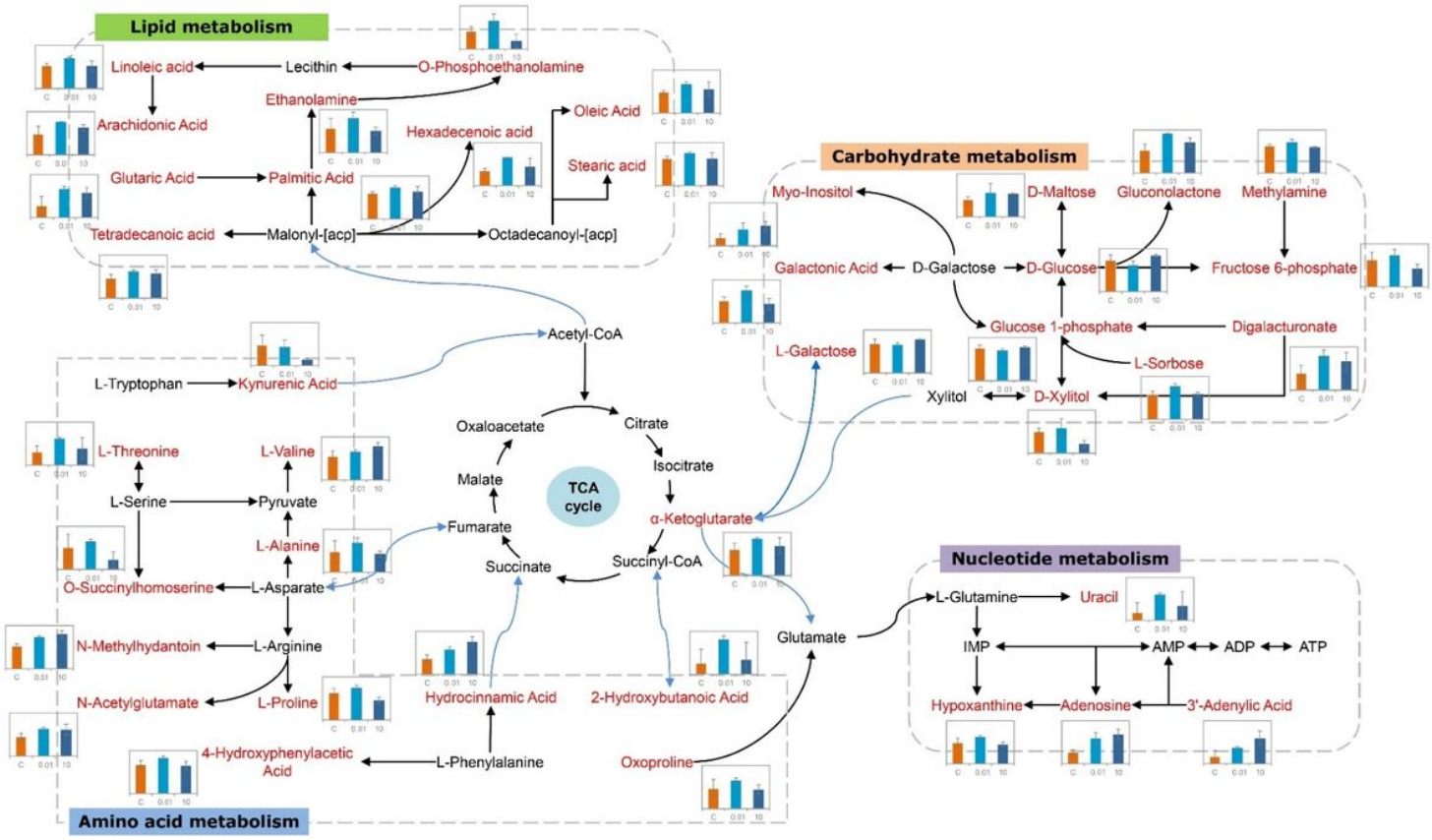

Figure 8

Metabolic pathway network map of significant altered metabolites of 0.01 mg/L, 10 mg/L GO-exposure, and control group. Metabolites identified in this study are shown along with a bar plot illustrating normalized concentration differences of metabolites in control group (saffron yellow bar), 0.01 mg/L GO-exposure group (light blue bar), and 10 mg/L GO-exposure group (dark blue bar). Red metabolites are significant differential, black metabolites not identified in this study.

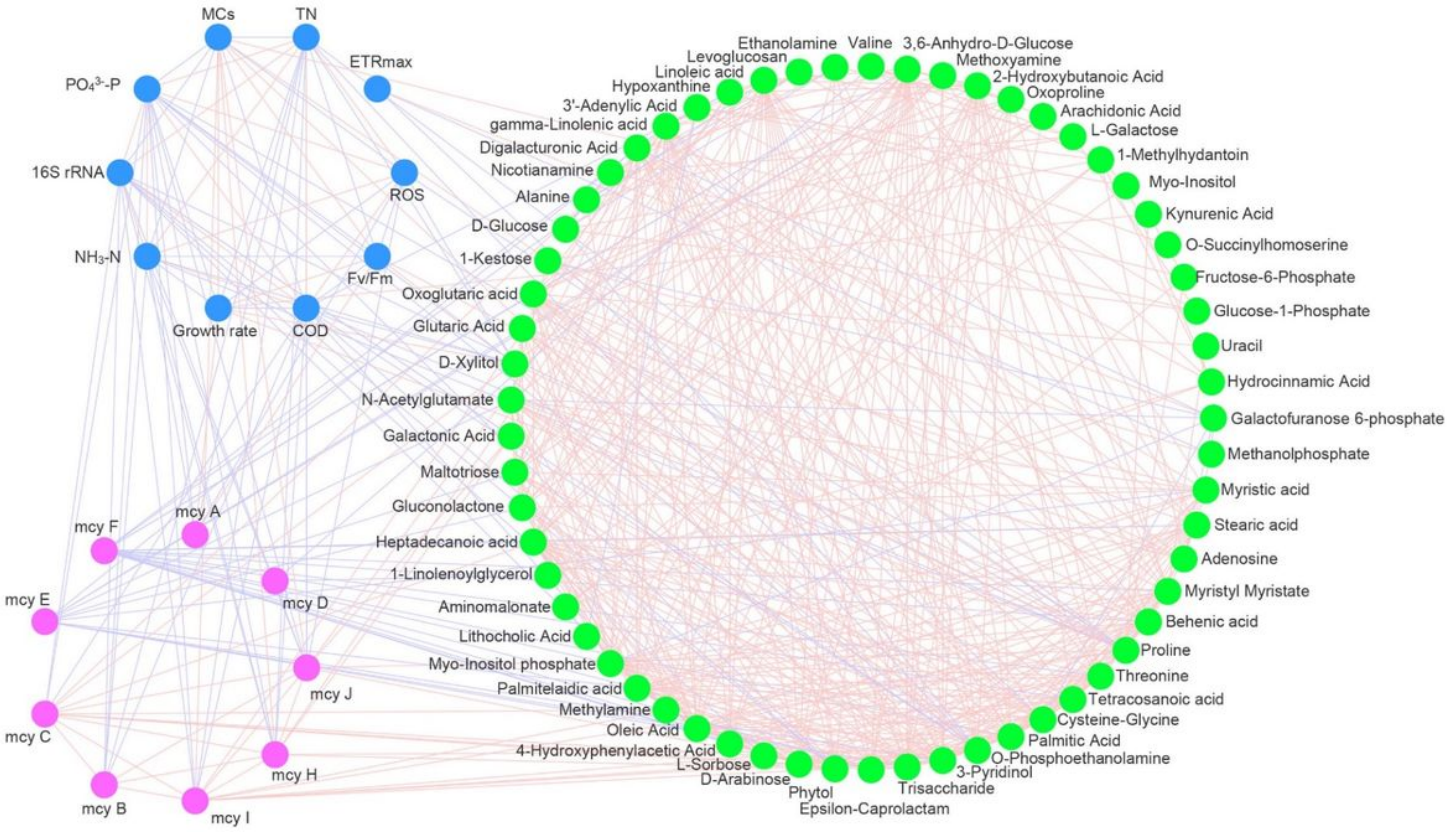

Figure 9

Pearson correlation network of metabolites (green), PO43−P, NH3-N, COD, ROS, Fv/Fm, ETRmax, growth rate, MCs, mcyA-J (red). The blue lines represent negative correlation coefficients, while red ones represent positive correlation. Only correlation coefficients significant at $p<0.05$ are considered ($|r| \geq 0.8$, FDR ≤ 0.05).

Supplementary Files

This is a list of supplementary files associated with this preprint. Click to download.

- Supplementarymaterials.doc